Pulsed Nd:YAG Laser Welding of Copper Using Oxygenated Assist Gases

E. BIRO, D.C. WECKMAN, and Y. ZHOU

The effects of using oxygenated assist gases on the weldability and weld properties of Nd:YAG, pulsed laser welds in copper (Cu) have been evaluated. It was found that the effective absorptivity of the Cu increased as the oxygen content of the Ar assist gas was increased. This facilitated laser welding of Cu at much lower laser powers and increased weld penetration. The use of oxygenated assist gas promoted nucleation and growth of submicroscopic oxide particles within the weld metal. These particles dispersion-strengthened the weld metal, thereby increasing both weld metal hardness and strength. However, when O_2 concentrations in the assist gas were greater than 90 pct, weld metal embrittlement due to excessive volume fractions of oxides was observed. The use of oxygenated assist gas also led to excessive cold lapping and poor bead quality. The bead quality was improved, however, by ramping-down the laser power before terminating each pulse.

I. INTRODUCTION

PROPERTIES such as high electrical and thermal conductivity, high ductility, high melting temperature, and corrosion resistance, make copper (Cu) an excellent material choice for many applications, such as electronic interconnections,[1,2,3] heat exchangers,[4,5] and packaging material.[6] However, some of these properties make Cu difficult to join. While brazing or soldering can be used to join Cu, these joints can be brittle, have high thermal and electrical resistivities, and have low melting temperatures. These are undesirable characteristics in microelectronic and heat exchanger applications and can inhibit the use of Cu for some applications. Laser welding can be an ideal process for joining Cu without the drawbacks of brazing and soldering because very precise, autogenous fusions welds can be made with very localized heating. However, Cu has a very low absorptivity to laser light and a high thermal conductivity. These properties make it difficult to laser weld Cu because most of the incident laser light is reflected off the surface of the Cu, and the small fraction of energy that is absorbed is very quickly conducted into the surrounding Cu substrate.

There are two basic approaches that have been used to improved the weldability of Cu by lasers. In the first approach, the incident laser power is simply increased until sufficient energy is absorbed to produce a weld. However, this requires very high-power lasers. In the second approach, the effective absorptivity of the Cu is increased so that the Cu absorbs a higher fraction of the incident laser power. In this case, welding is possible using much lower laser powers.

Lechuga *et al.*[7] and Ramos and Lechuga[8] have welded Cu with high-power, continuous wave (CW), Nd:YAG lasers. In these cases, the laser power used was sufficient to attain keyhole-mode welding conditions. Keyhole-mode welding has the added benefit that the effective absorptivity is increased to 90 pct or more due to the beam trapping effect of the keyhole.[9] In these studies,[7,8] the resultant solidification microstructures were examined, and weld strengths were measured; however, no work was done to characterize the physics of the joining process. In related work, Gouveia *et al.*[10–13] analyzed the joining kinetics during laser welding of Cu when using high-power, CW CO_2 lasers. They argued that CO_2 laser welding of Cu was only possible provided that sufficient energy was absorbed from the laser beam to ablate the Cu and form a plasma plume above the workpiece. They suggested that coupling was increased by inverse Bremstrahlung absorption[13] and argued that welding of Cu using CO_2 lasers was not possible without this mechanism. Because inverse Bremsstrahlung is a time-dependent mechanism,[9] Gouveia *et al.* predicted that laser welding of Cu is not possible with low-powered, pulsed Nd:YAG lasers.

Although high-power lasers can be used in welding of thick plates, in microlaser welding of thin sheets and wires for electronic and medical applications, high-power CW lasers are generally not used. This is because these lasers introduce excessive heat into the weldment, which can damage nearby heat-sensitive components. Low-power, pulsed lasers are favored instead for these joining applications because they can provide, during each pulse, the high peak power required for effective energy coupling between the laser beam and the Cu while maintaining a much lower, mean laser power. This facilitates welding while minimizing collateral heat damage of nearby heat-sensitive components.

The weldability of Cu with low-power lasers has been further improved using techniques that increase the effective absorptivity and coupling between the material and the laser beam. These techniques include using O_2 as an assist gas to promote oxide formation during welding and precoating of the Cu workpiece with a metallic or oxide coating prior to welding.[5,14–16] Oxidizing or plating the Cu surface increases the absorptivity of the workpiece, thereby improving energy coupling between the laser and the workpiece. This permits welding of Cu while using much lower laser powers.

Dell'Erba *et al.*[14,15] explored the use of O_2 as an assist gas when welding Cu with CW CO_2 lasers, while Daurelio and Giorleo[16] have examined further the effects of using

E. BIRO, Research Engineer, D.C. WECKMAN, Professor, and Y. ZHOU, Assistant Professor, are with the Department of Mechanical Engineering, University of Waterloo, Waterloo, ON, Canada N2L 3G1. Contact e-mail: nzhou@mecheng1.uwaterloo.ca

Manuscript submitted September 6, 2001.

O_2 assist gas when welding with both CW CO_2 and pulsed Nd:YAG lasers. With this technique, a thin oxide layer is formed on the weld pool surface during welding, which significantly improves the effective material absorptivity. This makes it possible to make keyhole-mode welds in Cu at much lower power densities. However, Daurelio and Giorleo[16] observed that the Cu weld metal contained oxide inclusions and suggested that these would decrease the material strength. On the other hand, Dell'Erba *et al.* observed no hardness difference between that of the base and the weld metal. Both researchers observed significant weld porosity.

Dell'Erba *et al.*[14,15] reported that CW CO_2 welding was not possible if the Cu was oxidized prior to welding with an inert assist. In subsequent work, however, Daurelio and Giorleo[16] and Shimizu and Hashimoto[5] reported successful laser welding of Cu after precoating the Cu with various materials. Daurelio and Giorleo evaluated the effectiveness of a variety of oxides, electrolytically plated Cr, and graphite, whereas Shimizu and Hashimoto[5] examined the effects of different thicknesses of electroless Ni plating. In both cases, there was little mention of how the plating changed the weld microstructure compared to the microstructure of a weld in unplated material.

While previous studies have shown that laser welding of Cu is possible with very high-laser powers or with application of various surface coatings to improve the absorptivity of the Cu during welding,[5,7–16] the effects of these joining techniques on joint properties and metallurgy have not been examined in detail. Also, although the occurrence of various weld defects, such as porosity and poor surface quality, have been noted in these previous studies,[12,14–16] there has been no work done towards identifying techniques that could be used to reduce or eliminate these defects. For example, Bransch *et al.*[17] and Matsunawa *et al.*[18] have shown that temporal pulse shaping of the laser pulse can significantly reduce or eliminate the severity of various weld defects in 304 stainless-steel, laser seam welds. The effects of temporal pulse shaping on weld defects observed in laser welded Cu have not been studied. In the present study, therefore, different techniques that might be used to increase the laser weldability of Cu using a low-power, pulsed Nd:YAG laser were investigated. The objectives of this work were to identify and develop techniques that will facilitate welding of Cu with a low-powered, pulsed Nd:YAG laser welder and to evaluate the effects of using these techniques on weld properties and weld microstructures. Finally, the effect of temporal pulse shaping on weld defects and weld quality was examined.

II. MATERIALS, EQUIPMENT, AND METHODOLOGY

A. *Materials and Sample Preparation*

The material used is this study was C11000 electrolytic tough-pitch Cu in the full-annealed condition. The nominal composition of this alloy was 99.9 wt pct Cu with 0.04 wt pct O. Base metal properties may be found in Table I. All samples were cut into 40 × 10 mm coupons with a shear before welding. Sheet thickness and further specimen preparation depended on the experiment conducted.

B. *Equipment and Fixturing*

All laser seam welds were made using a Lumonics (GSI Lumonics, Farmington Hills, MI) JK702H pulsed Nd:YAG laser with a 600-μm-diameter, fiber-optic beam delivery system. This laser was capable of up to 350 W mean power, 0.5 to 20 ms pulse widths, peak pulse powers up to 5000 W, and up to 55 J/pulse. The system had a 200-mm collimator lens and a 120 mm focal lens. The intensity distribution of the laser beam was measured with a rotating-wire-type laser beam analyzer and was found to be well described by a Gaussian distribution with a $1/e^2$ spot size of 413 μm. The internal laser-energy meter was calibrated with an Ophir Optronics (Ophir Optronics Ltd., Jerusalem, Israel) 1000 W laser power/energy meter, so all of the power and energy values reported are those at the material surface.[19] The nominal power density was calculated using the relation

$$PD = \frac{4P_p}{\pi w_0^2} \times 1000 \qquad [1]$$

where PD is power density (GW/m^2), P_p is peak power (W), and w_0 is the $1/e^2$ beam diameter (μm).

To avoid back-reflection, the laser head was aligned so that the incident laser beam was 15 deg to the normal of the sample (Figure 1). An assist gas was blown onto the sample surface using a 5-mm-diameter assist gas nozzle. The assist gas was composed of Ar with different concentrations of O_2. To obtain a measure of the relative effect of using the assist gas on the effective absorptivity of the Cu samples, the beam was reflected off the sample into an Ophir Optronics 1000 W laser power/energy meter, as shown in Figure 2.

C. *Experimental Procedures*

1. *Weld penetration tests*

Two tests were performed to examine the effect of various welding parameters on weld penetration. The first test series was a factorial experiment in which the effects of peak power, assist gas composition, weld speed, and pulse width on weld penetration into two 200-μm-thick Cu sheets in the lap-joint configuration were measured. In the second test series, the effects of peak power and assist gas composition on weld penetration were examined by making a series of bead-on-plate welds in an 800-μm-thick Cu sheet. All samples were washed in acetone, followed by a methanol rinse and air dried. After cleaning, the samples were immediately clamped under the beam in the required orientation and welded.

For the factorial experiment, the high and low values for each of the tested parameters were as follows: the welding speed was 1.25 or 2.5 mm/s, the assist gas O_2 content was either 20 or 80 pct in Ar, the pulse width was 3 or 7 ms, and peak laser power was 1390 or 2650 W. To characterize the variability of the system, four replicates were run with a welding speed of 1.875 mm/s, a 50 pct O_2-50 pct Ar assist gas, a pulse width of 5 ms, and a peak laser power of 2020 W. For the purposes of the statistical analysis, a semiqualitative penetration parameter was used to characterize the weld penetration, *i.e.*, the weld penetration was observed, and an integer number was assigned to the weld penetration parameter that was based on the number of sheets the weld penetrated. When the laser beam did not visibly mark the specimen surface, the penetration parameter was assigned a value of 0. Partial

Table I. Material Properties of C11000 Electrolytic Tough Pitch Cu[24,31]

Melting Temperature (°C)	Density (g/cm^3)	Specific Heat (J/kg °C)	Thermal Conductivity (W/m • K)	Absorbtivity of 1.06-μm Light at 25 °C (Pct)	Absorbtivity of 1.06-μm Light at 1085 °C (Pct)	Material Strength (N/mm)
1085	9.60	385	391	4.89	16.1	106.5

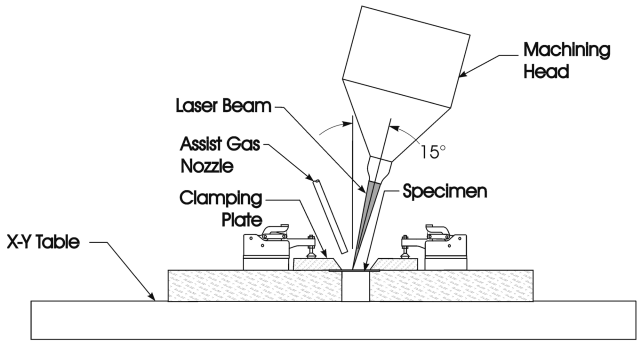

Fig. 1—Schematic of the welding jig used in the welding experiments.

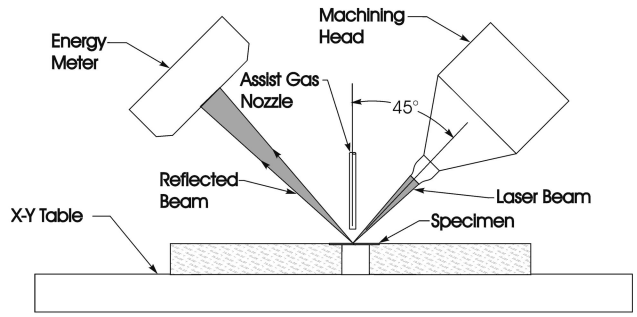

Fig. 2—Schematic of the jig used in the effective absorptivity ratio tests.

penetration into the top sheet was assigned a value of 1, and penetration into the second sheet was assigned a value of 2. When the laser penetrated both sheets, the penetration parameter was given a value of 3. In the one case where the experimental conditions were sufficient to cut through the material, the penetration parameter was assigned a value of 4.

During the second test series, the pulse width was 4 ms, the pulse frequency was 10 Hz, the assist gas flow rate was 15 lpm, and the welding speed was 1.25 mm/s. In these experiments, the laser peak power was varied.

2. *Absorptivity tests*

The absorptivity tests were designed to measure the relative effects of laser peak power, pulse width, and assist gas composition on the effective absorptivity of Cu. This was measured by projecting the laser beam onto the Cu specimen surface, as shown in Figure 2, and measuring the difference between the delivered beam power and the reflected beam power. To prepare the samples, the surface oxide was removed with BRASSO.* The samples were tested immediately following cleaning.

*BRASSO is a trademark of Reckitt & Colman Canada Inc., Toronto, and is a colloidal abrasive and chemical polishing solution commonly used for polishing Cu alloy articles.

The absorptivity tests were performed using peak laser powers ranging from 2000 to 4000 W and pulse widths ranging from 2 to 14 ms. For these tests, the pulse frequency was 5 Hz, and the sample speed was 6 mm/s. This combination of pulse rate and welding speed separated the individual laser spots on the material surface by 1.25 mm, ensuring oxide grown during the previous laser pulse would not affect the reflectivity measurement of the next laser pulse.

3. *Preoxidized Cu welding tests*

When the effect on weldability of preoxidizing the surface was tested, the specimens were first cleaned with BRASSO to remove any pre-existing surface oxide. They were then placed in a furnace with an air atmosphere at 700 °C for 10 minutes. After heating, they were furnace cooled to room temperature. This coated the samples with a 24.6 ± 1.8-mm-thick layer of CuO.[20] Once the samples were removed from the furnace, they were immediately welded. As in the weld penetration tests, the welding speed was 2.5 mm/s, the pulse frequency was 10 Hz, the pulse width was 4 ms, and the peak pulse power varied. In this experimental series, a 100 pct Ar assist gas flowing at 15 lpm was used.

4. *Tensile tests*

To measure the effect of assist gas composition on joint strength, 10-mm-long seam welds were made in a 500-μm-thick Cu sheet specimen in the butt-joint configuration and then tensile tested. The samples were prepared following the procedures used for the weld penetration tests. The samples were then welded using a welding speed of 2.5 mm/s, a pulse frequency of 10 Hz, and a pulse width of 4 ms. During welding, the peak power was set at the minimum power necessary to attain full penetration when welding in the butt-joint configuration. These conditions resulted in about a 58 pct overlap between individual spot welds. To shield the weld, various compositions of Ar-O_2 assist gas flowing at 15 lpm were used. By changing the welding peak power so that the weld pool dimension was held constant, the heat input into all of the welded specimens was kept constant regardless of assist gas composition used. This ensured that any differences in weld strengths were related to the effects of the use of different concentrations of oxygenated assist gas on the weld metal properties. After welding, the samples were punched using a 25-mm-diameter punch so that the width of the coupon at the weld would be reduced to 6 mm (Figure 3). Tensile tests were performed using an INSTRON* 4465 tensile tester with a 5-kN load cell. The samples were pulled so that the welds were perpendicular to the applied force. The crosshead speed was 10 mm/min. In this study, the tensile test results are presented in units of ultimate load divided by the width of the weld (N/mm). The strength of the base material was measured using the same apparatus as the tensile specimens.

*INSTRON is a trademark of Instron Corp., Canton, MA.

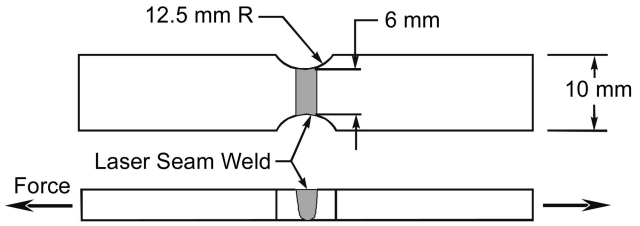

Fig. 3—Tensile specimen geometry of the 500-μm-thick laser seam welded Cu sheets.

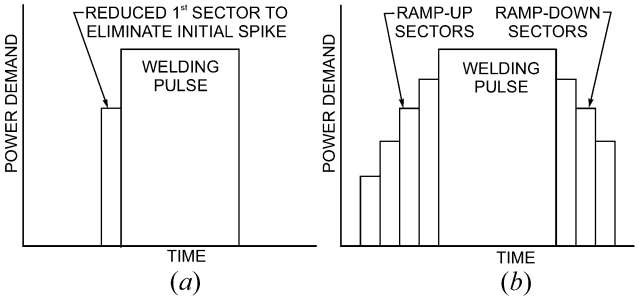

Fig. 4—JK702H flash lamp sector demand heights used to create different temporal pulse shapes: (*a*) 0.5 ms leading sector to eliminate initial power spike and (*b*) ramp-up or ramp-down sectors.

5. *Temporal pulse shaping*

A series of experiments were performed to explore the effects of temporal pulse shaping on weld defects in laser-seam-welded Cu. The same procedure used by Bransch *et al.*[17] to change the temporal pulse shape on the JK702H laser welder was used, *i.e.*, the laser pulse was broken into sectors, and the peak power and width of each sector was set. As may be seen in Figure 4(a), to eliminate the initial high-power spike[9] characteristically seen at the beginning of each pulse, an initial sector, 0.5 ms in duration and 63 pct of the height of the main welding pulse, was used. Ramped-up and ramped-down temporal pulse shapes were created by stepping the peak-power demand of a number of sectors preceding or following the main welding pulse (Figure 4(b)).

The power density of the welding section was set to deliver a power density of 25.2 GW/m^2 to the material surface. From previous tests, it was determined that this power density would create a bead in an 800-μm-thick sheet without penetrating the backside of the specimen. As before, the pulse width of the welding section was 4 ms. A minimum of three 0.3-ms sectors were used to make either the ramp-up or ramp-down sections, as this was the minimum number of sectors required to smoothly increase the laser power from 0 to the power of the welding sector. In the ramp-down section, the laser power was lowered from that of the welding pulse to 11.2 GW/m^2; this was the power below which no surface melting occurred. Examples of the laser output used in some of the experimental runs are shown in Figure 5.

6. *Optical metallographic procedures*

All optical metallographic specimens were mounted and polished to a 1-μm-diamond finish. They were then etched using an etchant consisting of 20-mL H_2O, 20-mL NH_4OH, and 10-mL H_2O_2. This was followed by a rinse with a 10-mL HNO_3 and 30-mL H_2O solution, a rinse in H_2O, an ultrasonic rinse in methanol, and finally, air drying. All photomicrographs and weld pool dimensions were obtained using a metallographic microscope.

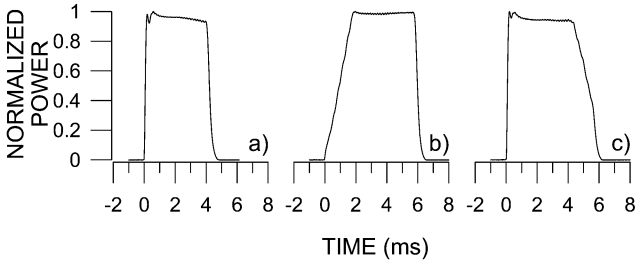

Fig. 5—Typical measured temporal power profiles for (*a*) top-hat pulse, (*b*) ramped-up pulse, and (c) ramped-down pulse.

Table II. Analysis of Variance Results from the Factorial Parametric Study

Variable	Effect	Mean Squared	*F* Value	Probability (Pct)
Speed	−0.875	3.06	12.3	3.95
Width	0.625	1.56	6.3	8.77
Peak power	1.125	5.06	20.3	2.05
O_2 (pct)	1.125	5.06	20.3	2.05
Interactions				
Speed and width	0.375	0.56	2.3	23.06
Speed and peak power	−0.125	0.06	0.3	65.14
Speed and O_2 (pct)	−0.625	1.56	6.3	8.77
Peak power and width	0.875	3.06	12.3	3.95
Width and O_2 (pct)	0.375	0.56	2.3	23.06
Peak power and O_2 (pct)	0.875	3.06	12.3	3.95
Error		0.25		

III. RESULTS

A. *Effect of O_2 on Laser-Material Coupling*

To study the effects of changing welding speed, pulse width, peak power, and assist gas O_2 content on weld penetration, a two-level factorial experiment was performed. The experimental results were analyzed statistically by comparing the variance associated with each variable. The analysis of variance (ANOVA) table allows comparisons to be made of the variance observed by changing main effects and interactions with the variance inherent to the experiment; this comparison is quantified by the F value. The higher the F value, the more likely that the observed variance was caused by changes to the independent variables not the normal variability inherent to the experimental results.

The results of the ANOVA analysis, complete with the probabilities of the various F values occurring, are shown in Table II. The error or variance inherent to the experiment was assessed based on the results of four replicate welding experiments. All of the main effects and interactions that had a probability of less than 10 pct were deemed significant. A visual representation of these effects can be seen in Figures 6 and 7. As may be seen, weld penetration was strongly dependent on welding speed, peak power, and assist gas O_2 content and weakly dependent on pulse width. An increase in all parameters tested, with the exception of welding speed,

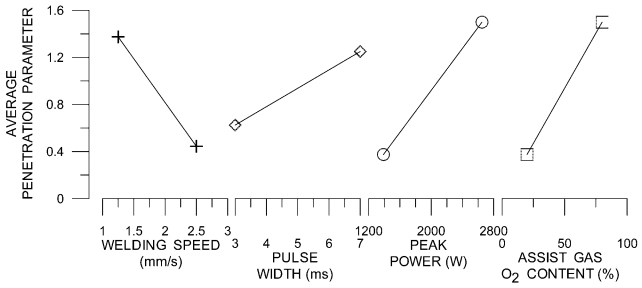

Fig. 6—Effect of welding speed, pulse width, peak power, and assist gas O_2 content on average weld penetration parameter.

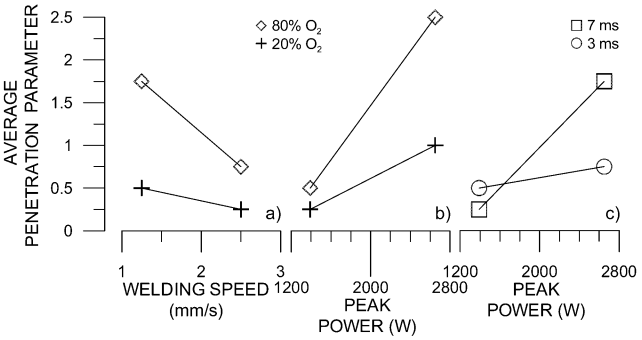

Fig. 7—Interactions between (*a*) welding speed and assist gas O_2 content, (*b*) peak power and assist gas O_2 content, and (*c*) peak power and pulse width.

caused an increase in weld penetration. Weld penetration decreased with increased welding speed. Also, as shown in Table II and Figure 7, three interactions were found to have significant effects; these were the interactions between speed and assist gas O_2 content, peak power and assist gas O_2 content, and peak power and pulse width. The effect of peak power on penetration was increased at high O_2 content and pulse width. Increasing O_2 content had a similar effect on reducing welding speed.

The relationships between peak power, assist gas composition, and penetration were tested by measuring the penetration of bead-on-plate welds produced with various peak power and assist gas compositions. As may be seen from Figure 8, welds made with a higher O_2 content in the assist gas had much greater penetration. In addition, the rate of increase of weld penetration with increasing power density increased rapidly with increasing O_2 content in the assist gas. The increased weld penetration indicates that an oxygenated assist gas increases the beam-material coupling efficiency. This confirms that the use of O_2 in the assist gas increases coupling between the laser beam and the workpiece. The increase in coupling was likely due to copper oxide growth on the material surface during welding.

Absorptivity tests were carried out using the experimental setup illustrated in Figure 2 in order to compare laser-material coupling between laser welds made with O_2 assist gas and Ar assist gas. The results are presented in Figure 9 as a ratio of the measured absorptivity of the material when using 100 pct O_2 assist gas over the measured absorptivity of the material with 100 pct Ar assist gas, *i.e.*, A_{O_2}/A_{Ar}. This provides an indication of how much the absorptivity increased through use of an O_2 assist gas. The measured

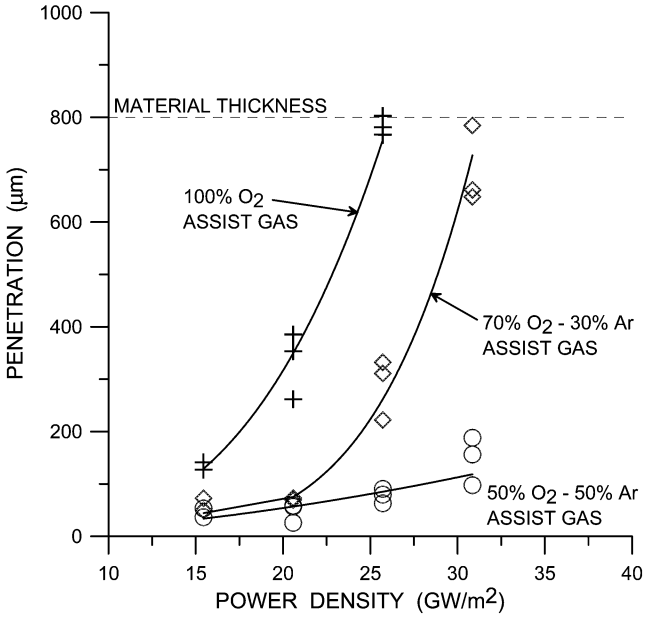

Fig. 8—Penetration of bead-on-plate welds with 100 pct, 70 pct, and 50 pct O_2 in Ar assist gases.

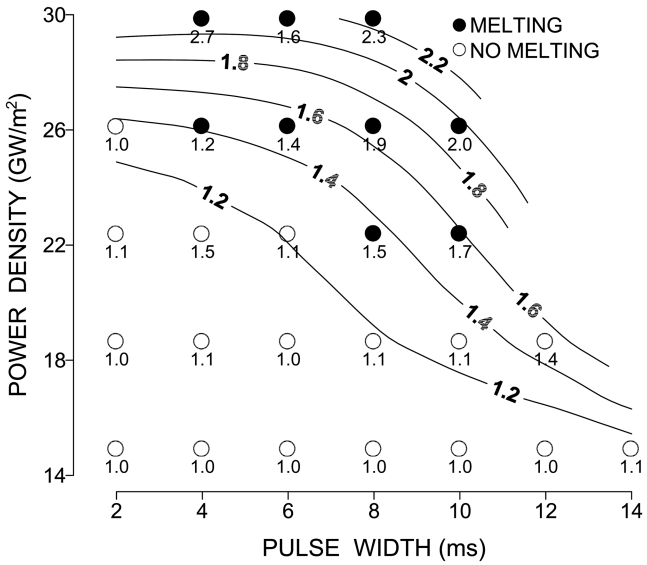

Fig. 9—Ratio of the effective absorptivity of Cu to 1.06-μm wavelength light when a 100 pct O_2 assist gas is used to that when a 100 pct Ar assist gas is used *vs* pulse width and power density.

absorptivity values are not presented, as there is a bias due to the experimental procedure used that is included in these measured values. It is assumed, however, that the biases for the measurements made with both assist gases are equal, so its influence is cancelled when the absorptivity ratio is calculated.

As may be seen in Figure 9, using 100 pct O_2 instead of 100 pct Ar assist gas increased laser energy absorption by the Cu by up to 2.3 times when melting occurs in the material. However, the increase in absorptivity is a function of pulse power and pulse width. The ratio of energy absorbed with an O_2 assist gas compared to that absorbed with an Ar assist gas increases as pulse power and pulse width increases.

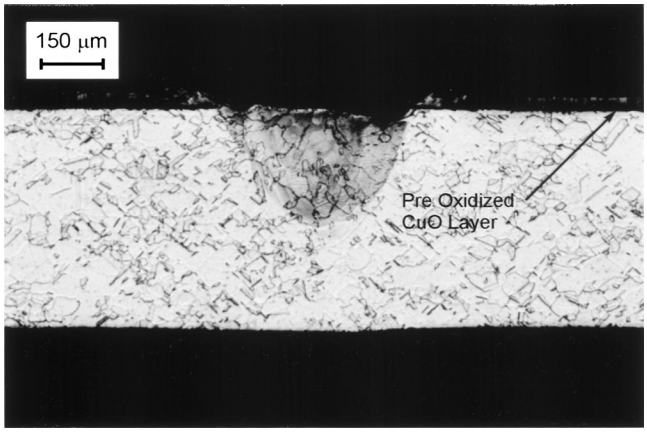

Fig. 10—Transverse section of a conduction-mode weld made in preoxidized Cu.

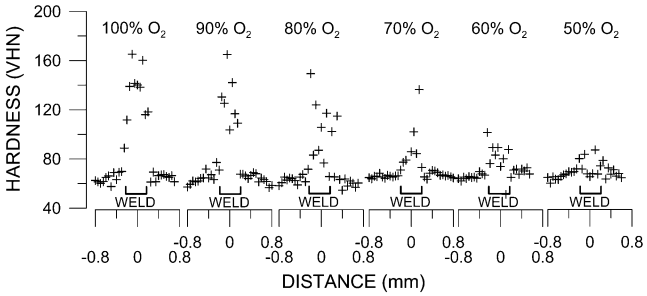

Fig. 11—Hardness profiles across welded Cu butt joints made with 100, 90, 80, 70, 60, and 50 pct O_2 in Ar assist gases.

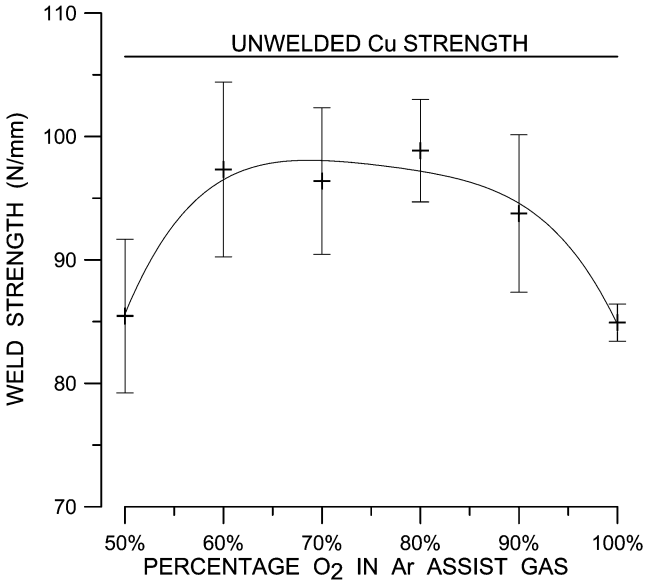

Fig. 12—Measured tensile strength of 500-μm-thick Cu butt-joints *vs* O_2 assist gas content (error bars are $\pm 1\sigma$).

However, there is a minimum power density ($\approx$18 GW/m^2) below which there was no significant increase in material absorptivity for the range of pulse widths tested. Again, this is an indication that the effective absorptivity is improved by oxide growth on the material surface. When either pulse power or pulse width is increased, more oxide can form on the material surface due to either higher surface temperatures or a longer growth time. If more oxide grows on the surface, the material can absorb more energy. Increasing either laser power or pulse width increases the effective absorptivity of Cu when an O_2 assist gas is used as compared to an Ar assist gas.

B. *Effect on Weldability of Predeposited CuO Surface Film*

It was found that full-penetration, laser seam welds could be achieved in a 500-μm-thick Cu sheet that had been precoated with a 25-μm-thick layer of CuO using the JK702H laser with Ar assist gas and different peak-pulse powers. Depending on the peak power used, these welds were either in conduction mode or keyhole mode. Figure 10 is a transverse section of a typical conduction-mode weld. Notice that the 25 μm CuO layer is no longer present on the surface of the weld. These results indicate that it is not necessary to continuously create a layer of oxide on the material surface to ensure the weld pool absorbs enough energy to grow if there is a highly absorptive layer on the surface of the workpiece.

C. *Weld Microstructure and Properties*

Microhardness profiles were made horizontally across weld sections of welds made in a clean Cu sheet using oxygenated assist gases while welding. As may be seen in Figure 11, the assist gas O_2 content had two significant effects on the weld metal hardness. As the O_2 content of the assist gas increased, both the hardness and the hardness variability increased.

The increase in weld metal hardness with increasing O_2 assist gas concentration is likely due to dispersion strengthening from small oxide inclusions introduced into the weld metal by the oxygenated assist gas. The variation in measured hardness within the weld pool indicates that the oxide distribution was not homogenous throughout the weld. This suggests that there was insufficient time for complete mixing of the oxides throughout the weld during each spot weld and that the inclusions are spread throughout the weld in a random manner, creating oxide-rich and oxide-poor regions.

The tensile strengths of the butt joints made in the 500-μm-thick Cu sheet were found to be a function of the assist gas O_2 composition (Figure 12). Compared to the measured base-metal strength of 107 N/mm, the joints welded with 100 pct O_2 assist gas had lower strengths of about 85 N/mm. However, as the O_2 content of the assist gas was reduced to between 60 and 80 pct O_2, the joint strength increased to a maximum of about 97 N/mm. This represents a joint efficiency of about 90 pct with respect to the fully annealed, C11000 Cu sheet strength. The joint strength decreased again to about 85 N/mm when the assist gas O_2 content was further reduced to 50 pct.

The fracture surfaces of the joints made with 100 pct O_2 and 60 pct O_2-40 pct Ar assist gas were examined after fracture (Figure 13). The fracture surface of the joint welded with 100 pct O_2, shown in Figure 13(a), had a relatively smooth fracture surface indicative of brittle fracture with cleavage as the fracture mechanism. Alternatively, the fracture surface of the joint welded with 60 pct O_2-40 pct Ar,

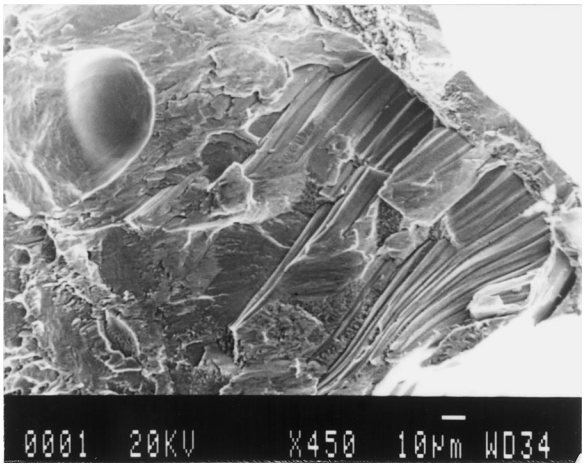

(*a*)

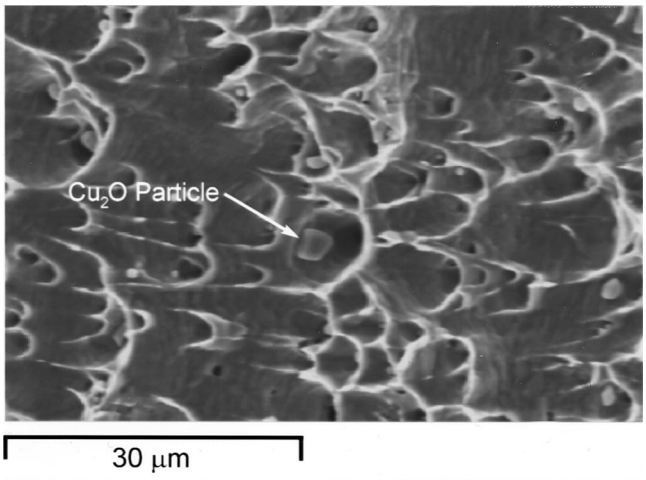

(*b*)

Fig. 13—Fracture surfaces from butt joints welded with (*a*) 100 pct O_2 assist gas and (*b*) 60 pct O_2-40 pct Ar assist gas.

shown in Figure 13(b), appeared very rough with a classical cup-cone morphology typical of ductile fracture. These fracture surfaces indicate that the fracture mode changed from ductile to brittle with increasing O_2 content in the Ar assist gas.

The high strength of the welds made with 60 to 80 pct O_2 assist gas indicates that dispersion strengthening by copper oxide inclusions has occurred. However, when 50 pct O_2 assist gas was used, the joint strength again dropped. The correlation between assist gas content and joint strength for the joints that failed in a ductile fashion match the data from the microhardness profiles shown in Figure 11. In these profiles, the hardness profiles of the welds made with an O_2-rich gas had high hardness, and the hardness dropped to that of the base metal for the welds made with 50 pct O_2 assist gas, where there would be fewer oxide particles in the weld metal.

It is evident from Figures 11 and 12 that the weld metal hardness and strength have increased significantly with assist-gas oxygen content. This would suggest that either sufficient oxide formed on the weld surface during welding has been drawn within and mixed into the weld pool by fluid flow in the weld pool during welding or that sufficient

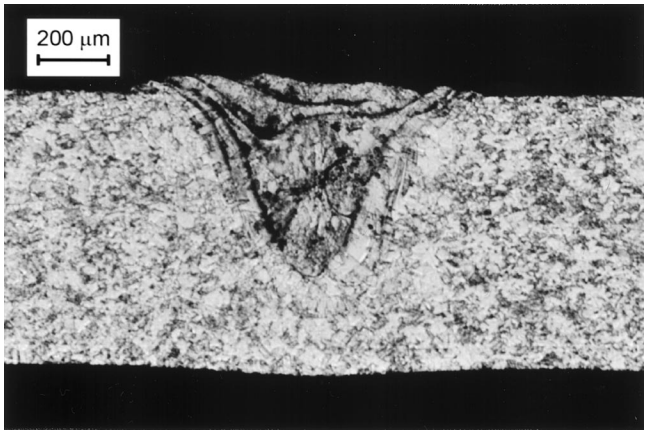

(*a*)

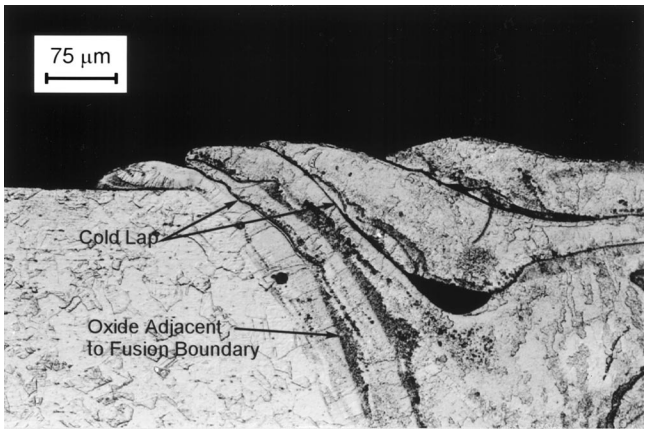

(*b*)

Fig. 14—Cross section of a weld made with a top-hat shaped pulse: (*a*) whole weld and (*b*) top right corner of the weld.

O_2 has been absorbed into the liquid during melting and sufficient Cu oxide inclusions formed within the weld metal to increase the hardness and strength of the weld metal by dispersion strengthening. As may be seen in the transverse section of a typical weld, shown in Figure 14, and in the longitudinal section of a typical weld, shown in Figure 15, Cu oxide inclusions were generally not evident in the bulk of the weld metal when viewed under an optical microscope; however, bands of coarse Cu_2O oxide particles[2] were frequently observed near the fusion boundary.

[2]Cu_2O has a ruby red color when viewed under polarized light.[21]

When the welds were examined by Field Emission Scanning Electron Microscope (FESEM), submicroscopic particles were observed in the microstructure. These particles were identified as Cu_2O by X-ray diffraction (XRD) analysis.[22] The elemental content of the welds with 100 pct O_2 and 50 pct O_2-50 pct Ar assist gas and the base material were measured ten times each at different locations within the weld metal using energy dispersive x-ray analysis. It was found that the welds made with 100 pct O_2 assist gas contained an average of 1.44 ± 0.40 ($\pm 1\sigma$) wt pct [O], the welds made with 50 pct O_2-50 pct Ar assist gas contained only 1.16 ± 0.21 wt pct [O], and an average of 1.00 ± 0.10 wt pct [O] was measured in the base material. A two-tailed statistical t-test was performed on the data. It was

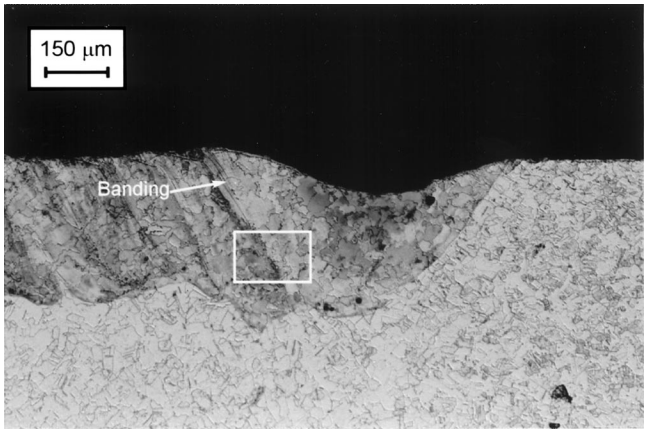

(*a*)

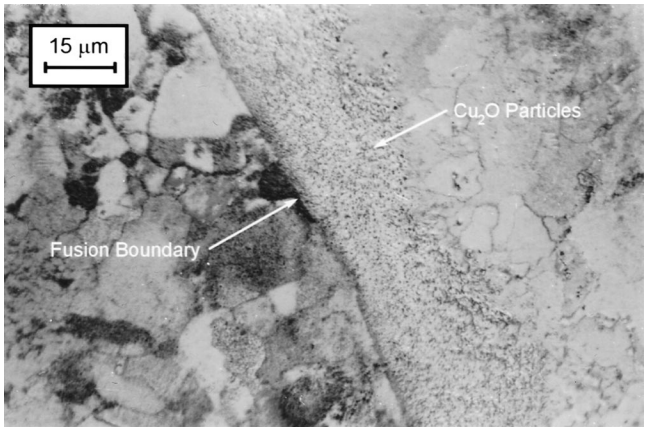

(*b*)

Fig. 15—Longitudinal section of pulsed laser bead-on-plate weld showing (*a*) the bead profile up to the last weld and (*b*) the fusion boundaries in the area indicated.

found that there was a 0.16 pct probability that the welds made using the 100 pct O_2 and the 50 pct O_2-50 pct Ar assist gas have the same mean oxygen content. Similarly, there was a 0.06 pct chance that the welds made using the 50 pct O_2-50 pct Ar assist gas and the base metal have the same mean oxygen content. These measured differences are large enough to indicate that the addition of O_2 to the assist gas can significantly affect the oxygen content in the weld metal, as the differences between the measurements with the two assist gas compositions and the base material are significant. The oxygen content of these materials correspond to 12.9 wt pct Cu_2O, 10.4 wt pct Cu_2O, and 8.9 wt pct Cu_2O, respectively. These oxides may be seen in Figures 13(b) and 14(b). Although the welds made with a preoxidized CuO surface layer were made using a 100 pct Ar assist gas, the oxygen content of these welds were 2.26 ± 0.34 wt pct [O] or 20.2 wt pct Cu_2O. This is significantly higher than was found in the welds made in clean Cu and 100 pct O_2 assist gas. The large amount of dissolved oxygen is probably due to the fact that the grown oxide was thick compared to the base material. These observations would suggest that the observed increases in weld metal hardness and strength was caused by dispersion strengthening due to submicroscopic Cu_2O particles throughout the weld metal.

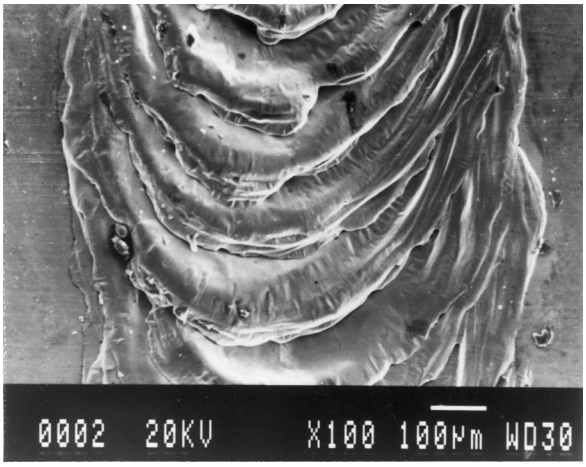

Fig. 16——Weld bead surface of a weld made with a top-hat temporal pulse shape.

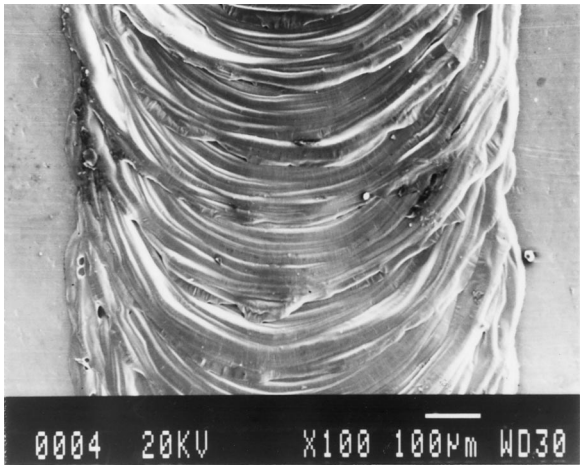

Fig. 17—Weld bead surface of a weld made with a ramped-down temporal pulse shape.

D. *Weld Defect and the Effects of Temporal Pulse Shaping*

As may be seen in Figures 14 and 16, the top surface of welds made with a 100 pct O_2 assist gas were very irregular with many cold laps, and there were a significant number of pores in the weld metal. By examining the welds under polarized light, Cu_2O was found in both the pores and the cold laps.

Following the work of Bransch *et al.*[17] and Matsunawa *et al.*,[18] the use of temporal pulse shaping for smoothing the weld surface profile and reducing the severity of cold laps and pores, such as those shown in Figures 14 and 16, was examined. As stated earlier and shown in Figures 4 and 5, the laser power was either ramped-up or ramped-down, following the rectangular welding pulse.

Ramping-up the power was found to have little effect on smoothing the weld surface or eliminating cold laps and oxide inclusions from the weld. Conversely, as may be seen in Figures 17 and 18, ramping-down the pulse before terminating the beam was found to significantly improve the weld bead quality and reduce the severity of cold lapping in the weld. As may be seen by comparing Figures 14(b) and 18(b),

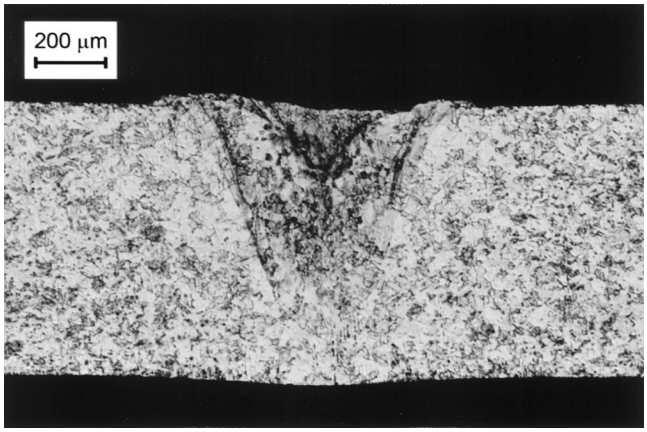

(*a*)

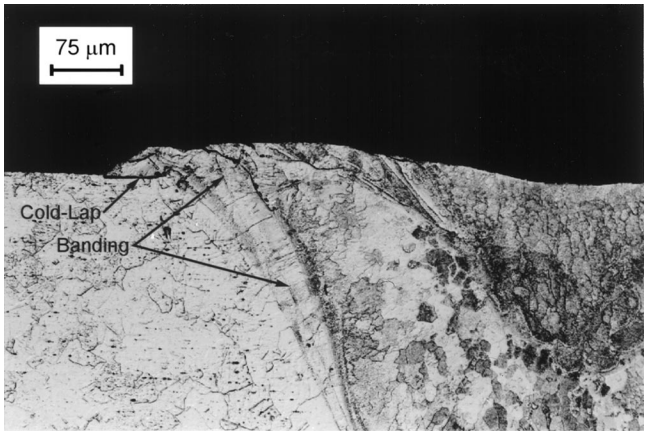

(*b*)

Fig. 18—Transverse section of a weld made with a 3.6-ms ramp-down pulse shape: (*a*) whole weld and (*b*) top left corner of the weld.

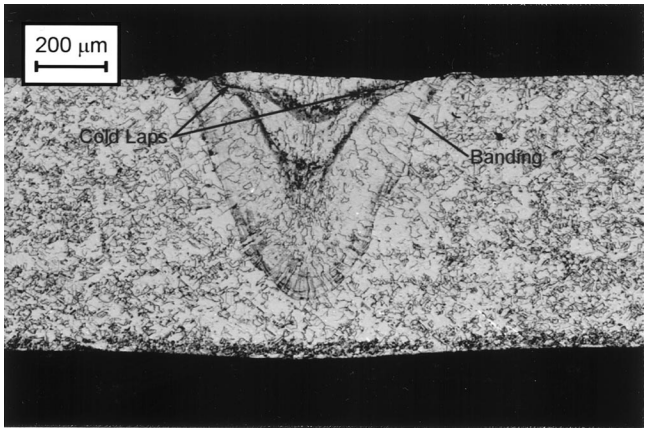

(*a*)

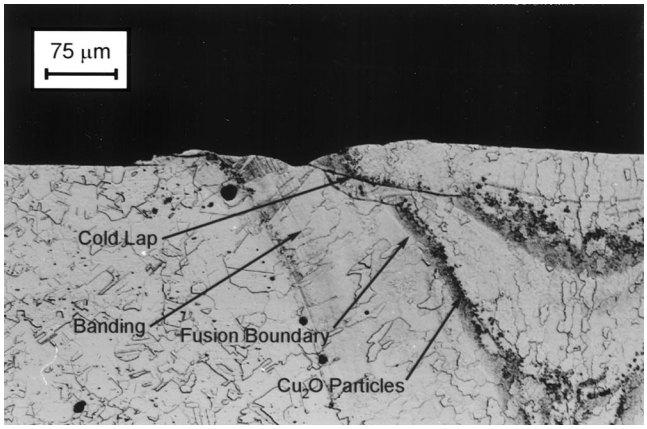

(*b*)

Fig. 19—Transverse section of a weld made with a 6.2-ms ramp-down pulse shape: (*a*) whole weld and (*b*) top left corner of the weld.

ramping the laser power down over a period of 3.6 ms after the main welding pulse greatly improved the weld quality by reducing the severity of cold lapping, although cold laps were not eliminated completely. However, when the pulse ramp down was increased to 6.2 ms, the severity of cold laps in the weld increased again (Figure 19). The increase in the severity of cold laps at long pulse times is probably due to the extensive time that Cu_2O had to build up on the weld pool surface during the cool down period. It should also be noted that moderate ramp-down times eliminated much of the porosity found in the welds made with top-hat pulses. Similar effects have been observed in stainless-steel laser welds.[17,18]

Although temporal pulse shaping almost eliminated the weld defects, a series of light and dark bands parallel to the fusion boundary formed in the weld metal microstructure in all of the welds produced with ramped-down pulse shape (Figures 18 and 19). By examining the dark bands under polarized light, it was determined that these bands contained dense arrays of small particles of Cu_2O. This microstructural feature was caused by a phenomenon known as banding, which can commonly be seen in laser solidified microstructures.[23] Banding is a transient variation in solute content at the solid/liquid interface caused by sudden changes in the instantaneous rate of solidification, such as would occur during the ramp-down portion of the laser pulse. Banding was not observed in welds made with a standard top-hat pulse shape or a ramped-up pulse shape because there were not sudden changes in solidification rates during the solidification of the spot welds.

IV. DISCUSSION

A. *Effect of O_2 on Laser-Material Coupling*

The increase in the average penetration parameter with the other significant, weld-process parameters and the interactions between these parameters observed in the factorial experiment results (Table II and Figures 6 and 7) is thought to be due to three root causes. The first is that by changing parameters, such as peak power and pulse width, the total energy transferred to the material is increased, and this results in more heating and melting. Also, with more energy transfer to the material, the material temperature will rise, and the growth rate of the surface oxide will increase, thereby increasing coupling efficiency and weld penetration in an autocatalytic fashion. Second, if welding speed is decreased, there will be more time for oxide growth, thereby increasing the oxide thickness and, in turn, increasing energy coupling efficiency and weld penetration. Finally, by increasing the assist gas O_2 content or partial pressure of O_2 over the weld surface, the rate of oxide growth will increase, again

resulting in improved energy coupling and greater weld penetration.

B. *Mechanisms for Improved Absorptivity*

As indicated in Figure 7, surface marking or melting was not observed in the Cu sheets when the assist gas contained no O_2 primarily because the absorptivity of C11000 Cu was too low ($A_{Cu} = 4.89$ pct), and the peak power of the JK702H laser welder was limited to 5000 W. However, when the O_2 concentration in the assist gas was increased, laser-material coupling increased sufficiently to melt the material and create a weld. This is similar to the results of Dell'Erba *et al.*[14,15] and Daurelio and Giorleo,[16] who found that using oxygen as an assist gas increased laser beam coupling with Cu. Weld penetration was also found to increase with the O_2 content of the assist gas. Again, this agrees with the current theory that the use of O_2 during laser heating will form Cu_2O,[24,25] which, because of its high absorptivity of 80 pct,[26] can better absorb energy from the laser than can the underlying Cu, which has an absorptivity of only 4.89 pct at 25 °C and 16.1 pct at its melting temperature of 1085 °C.[27]

Varying pulse power, pulse width, and assist gas composition can control the amount of Cu_2O formed on the weld pool surface. Changing the pulse width and the pulse power affects how much oxide is able to grow. If it is assumed that Cu_2O growth obeys Wagner's law,[25] then the rate of growth of the oxide, dx/dt, is described by the relation

$$\frac{dx}{dt} = \frac{d_0}{x} \exp\left(-\frac{T_D}{T}\right) \qquad [2]$$

where x is oxide thickness, t is time, d_0 and T_D are solid-state diffusion constants for the ions in the oxide layer, and T is absolute temperature. From Wagner's law[25] (Eq. [2]), as temperature increases, the rate of oxide growth increases exponentially, but as growth time increases, the oxide only grows by the square root of the increase in time. The peak pulse power controls the temperature of the Cu surface, and the pulse width controls the amount of time that the oxide has to grow. Liu and co-workers[28,29] have shown that following an initial transient during the first 2 to 4 ms of laser spot welds in aluminum and stainless steel, respectively, conduction of heat into the underlying base metal limits the rate of increase of weld dimensions and weld temperatures, whereas weld dimensions and temperatures remain strongly dependent on the power density of the incident laser beam. This would suggest that following the initial transient in the Cu welds, the rate of growth of oxide on the weld pool surface will increase approximately as the square root of the pulse time but that there will be an exponential increase in the oxide growth rate with increasing laser-power density.

Increasing the O_2 content of the assist gas was also found to increase energy-coupling efficiency and weld penetration. This is because changing the composition of the assist gas changes the partial pressure of O_2 in contact with the Cu surface. This allows more O_2 to react with the Cu surface, thus forming a thicker layer of Cu_2O. After melting occurs, Cu_2O is constantly being mixed into the weld pool by the fluid flow. Although the absorptivity of the weld pool should increase slightly as Cu_2O is mixed within the weld and the volume fraction of Cu_2O in the liquid is increased, the change in absorptivity would still be expected to be too low to have a significant impact on the rate of weld pool development. To maintain high surface absorptivity, therefore, oxide must be continually formed at the surface, as the thickness of oxide at the surface has the largest effect on increasing absorptivity.

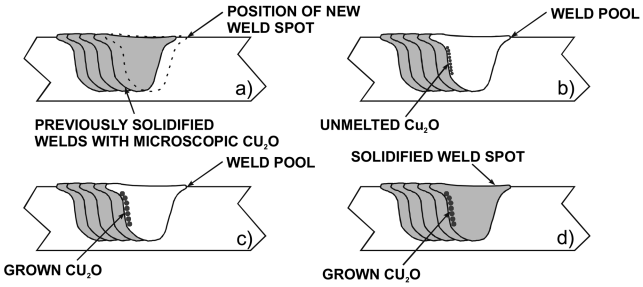

Fig. 20—Schematic of a longitudinal section of a laser seam weld and the stages of oxide growth near the trailing edge of the new spot weld: (*a*) sketch of previous welds; (*b*) new weld pool is made, but microscopic oxide at edge of weld does not melt into the weld pool; (*c*) the unmelted oxides grow by diffusion; and (*d*) the larger oxide particles are trapped in the solidification structure when the weld pool solidifies.

During experimentation, it was found that reducing welding speed allowed melting to occur in the material when the O_2 content of the assist gas was too low to allow welding at higher speeds. As welding was done using a pulsed laser, slowing the welding speed increased the pulse overlap. As may be seen in Figure 20, each new pulse does not need to build up oxide and melt a spot in unoxidized material, instead previous laser pulses have already oxidized the majority of the material being exposed to the beam. So, in the case of this study, where most of the welding was done using a 4 ms laser pulse, the surface will not only grow an oxide for 4 ms, but in each laser pulse, some of the material surface being irradiated by the laser will have had 4 ms to grow an oxide, some of the surface will have grown the oxide for 8 ms, some of the surface will have grown the oxide for 12 ms, etc. The larger the pulse overlap, the longer the oxide is allowed to grow on the weld bead surface, and the more the effective absorptivity will increase. This was the observed behavior when the welding speed was slowed. Slowing the welding speed increases the pulse overlap, indirectly increasing the oxidation time, and thus improves beam-material coupling.

The measured, effective-absorptivity ratios, A_{O_2}/A_{Ar}, shown in Figure 9, are lower than might be expected based on ratio of the absorptivities of pure Cu_2O and Cu. The absorptivity of Cu_2O is 80 pct[26] and the absorptivity of molten Cu is only 16.1 pct.[27] This gives a theoretical absorptivity ratio of about 5. The maximum A_{O_2}/A_{Ar} ratio measured in this study was only 2.3 (Figure 9). It must be remembered, however, that the absorptivity values for pure Cu_2O and Cu are measured under steady isothermal conditions, while the effective-absorptivity measurements obtained in this study using the apparatus shown in Figure 2 represents a time-averaged effective absorptivity. When the laser pulse first begins, there is no oxide present on the Cu surface, and the effective absorptivity is that of pure Cu, *i.e.*, only 4.89 pct at room temperature increasing to 16.1 pct at the melting temperature of Cu.[27] As the surface is heated, the rate of oxidation increases exponentially with temperature (Eq. [2]). When the thickness of the oxide film exceeds $^1/_4\ \lambda$ of the laser light, or ≈270 nm,[30] the oxide film will begin to absorb

the light rather than the underlying Cu, and the effective absorptivity can be expected to increase quickly to that of pure Cu_2O, *i.e.*, 80 pct.[26] This will cause rapid heating of the oxide film, and initially, this heat will be conducted directly to the underlying Cu, causing rapid heating and melting of the Cu. The oxide has a low thermal conductivity and, when subjected to the high power density of the laser beam, will heat up very quickly to temperatures above its melting temperature of 1242 °C.[31] The molten layer of oxide will continue to absorb light and to increase in temperature until it reaches its boiling temperature of 1800 °C;[31] at which point, the oxide will vaporize, leaving behind the low absorptivity molten Cu. Thus, in the final stages of the laser pulse, there can be expected to be a variation in absorptivity over the surface of the weld pool from low absorptivity of molten Cu in the center of the weld pool and the Gaussian-distributed laser beam to a ring of higher absorptivity molten Cu_2O, followed by solid Cu_2O, as one moves further away from the center of the laser beam, where the incident power density is much lower. Both the temporal variation of absorptivity and spatial variation of absorptivity during the final stages for the laser pulse will contribute to decreased measured values of the effective-absorptivity ratio from the theoretical value of about 5 to the maximum values of about 2.3 measured in this study using the apparatus shown in Figure 2. Irrespective, this increase in effective absorptivity was sufficient to allow laser welding of the Cu sheets using the low-powered, pulsed Nd:YAG laser welder.

C. *Oxide Inclusions in the Welds*

In all of the welds made with the O_2-based assist gas, layers of Cu_2O were observed at the interface between the cold laps (Figure 14(b)), and clusters of large Cu_2O particles were observed adjacent to the fusion boundaries with other pulses (Figures 15 and 19). As well, submicroscopic particles of Cu_2O were detected in the weld microstructure. These submicroscopic Cu_2O precipitates were responsible for dispersion strengthening of the weld metal and the measured increases of both the hardness and the strength of the weld metal.

The large Cu_2O particles seen near the fusion boundaries of individual pulses are formed by different mechanisms than the Cu_2O precipitates in the weld metal. These large oxide particles were only formed when previously oxygenated material was remelted and resolidified, as shown schematically in Figure 20. When the weld pool originally solidifies, it is filled with submicroscopic oxides (Figure 20(a)). When the next laser pulse melts the material for the new spot weld, the previously welded Cu-Cu_2O weld metal alloy is melted to form the new weld pool. However, as the melting temperature of Cu_2O is 1242 °C,[31] slightly higher than that of Cu (1085 °C[32]), the Cu_2O at the edge of the weld pool remains unmelted (Figure 20(b)). Because the unmelted oxide is in the unmixed zone at the edge of the weld pool, it is not swept into the center of the weld pool, where it would remelt. At the edge of the weld pool, these particles are exposed to elevated temperatures that allow them to grow by diffusion (Figure 20(c)). When the weld pool solidifies, these larger oxides are trapped adjacent to the fusion boundary of the pulse (Figure 20(d)). These oxides are too large to significantly affect the bulk weld properties.

The submicroscopic oxides detected within the weld altered the joint strength of the Cu welds. From Figure 12, it can be seen that there is a reduction in tensile strength as the O_2 content of the assist gas is increased above 90 pct because of embrittlement of the weld metal and the resultant transition from ductile to brittle fracture behavior. However, the tensile strength of the joints made with an assist gas containing between 60 and 80 pct O_2 had an average tensile strength of 97.5 N/mm, which is 91.5 pct of the base material strength. These joints have strengths greater than those measured by Lechuga *et al.*,[7] who measured joint strengths that were 81 pct of the base material strength in welds made without O_2 assist gas. Thus, if a weld contains a moderate amount of oxide, the weld metal is dispersion strengthened. The welds made with 50 pct O_2-50 pct Ar assist gas had an average joint strength of 85.5 N/mm or 80.2 pct of the base metal strength. The strengths of these welds are comparable to those measured by Lechuga *et al.*[7] However, there was not sufficient oxide content in these welds to cause significant dispersion strengthening. As the volume fraction of submicroscopic Cu_2O precipitates increases, the strength of the weld metal will increase at the expense of ductility until, finally, a transition from ductile to brittle behavior occurs, as seen in Figure 13.

D. *Effect of O_2 on Fluid Flow and Weld Pool Shape*

When welding with an O_2-rich assist gas, there was generally larger scatter in hardness measurements, rougher bead-surface profiles, and larger numbers of cold laps. These defects became more severe as the O_2 content of the assist gas was increased. However, the severity of these defects was reduced when the pulse power was ramped-down before terminating the pulse. Elimination of porosity through the use of a decaying pulse was reported by Bransch *et al.*[17] and Matsunawa *et al.*[18] when working with stainless-steel laser welds. In these cases, pulse shaping was used to control the collapse of the keyhole to prevent metal vapor from being trapped in the molten pool, thereby forming occluded vapor pores. In the present work, it is believed that ramping-down the pulse also prevents gas from being trapped in the Cu weld pool, but instead of metal vapor, the gas is O_2 evolving from the solidification front during solidification. When the weld pool solidifies, oxygen in excess of the solubility limit of [O] in Cu is rejected back into the liquid at the solid/liquid interface. As the concentration of [O] increases, bubbles of O_2 will nucleate and grow large enough to break away from the interface and rise out of the weld pool. If solidification occurs rapidly, as when a top-hat temporal pulse shape is used, the high rate of oxygen evolution will increase mixing in the weld pool and also cause significant disturbance and splashing of the free surface of the weld pool as the O_2 bubbles break the surface. This disturbance results in excessive cold lapping and a rough bead surface. If the weld solidifies more slowly, as happens when a ramped-down temporal pulse is used, oxygen will evolve from the weld pool at a much slower rate, and most of the oxygen will escape before solidification occurs, resulting in less disruption of the free surface. Thus, the weld pool will solidify with improved bead quality.

While temporal pulse shaping improved the final bead profile and reduced the severity of cold lapping, cold lapping was not completely eliminated. At the edge of the weld bead, on either side of the weld, some thin cold laps were

still found. Although the cold laps did not go across the entire weld width, they could still act as stress concentrations.

V. SUMMARY AND CONCLUSIONS

During pulsed Nd:YAG laser welding of Cu, it was found that oxygen was needed in the atmosphere above the weld pool in order to facilitate laser welding of Cu using a low-power, pulsed Nd:YAG laser, *i.e.*, welding was not possible using the power available from the Lumonics JK702H laser welder used in this study and only Ar assist gas over the Cu. Oxygen from the assist gas formed a highly absorptive oxide layer that greatly improved laser beam coupling with the Cu workpiece. When coupling was increased, the workpiece could absorb significantly more energy, thus facilitating melting and formation of a weld pool. Weld penetration was also found to increase with increased O_2 content in the Ar assist gas or with decreased welding speed when using oxygenated assist gas. Both of these changes promote rapid oxide growth on the weld pool surface during welding, thereby increasing the effective absorptivity of the weld pool and, thus, the energy absorbed during each laser pulse.

Use of the O_2-Ar assist gas did not lead to a loss of joint strength over most of the range of O_2 concentrations used. Reduced joint strength was only noticed in the welds made with an assist gas containing between 90 and 100 pct O_2. The fracture surface of these welds indicated the joints failed in a brittle manner. However, the welds made with an assist gas containing between 60 and 80 pct O_2 had strengths higher than those of oxygen-free welds. The increase in strength is due to dispersion strengthening of the weld metal by Cu_2O precipitates introduced through use of the O_2-rich assist gas. The fracture surface of these welds indicated failure occurred in a ductile fashion. When 50 pct O_2 assist gas was used, joint strength dropped to strengths comparable to welds made without O_2 assist. In these welds, there were insufficient oxides to strengthen the weld.

Welds made with square (top-hat), temporal pulse shapes generally had gas pores, cold laps, and poor bead quality. These defects were attributed to weld surface turbulence caused by excess O_2 gas bubbles rising from the weld pool during solidification. When the laser power was moderately ramped-down, however, these defects were minimized. The weld quality improved due to a combination of less rapid evolution of O_2 from the weld and a slower solidification rate. The less rapid evolution of O_2 resulted in the weld pool being less turbulent, and the slower solidification rate allowed the weld surface to calm before freezing.

ACKNOWLEDGMENTS

The authors thank the Edison Welding Institute (Columbus, OH) for supporting this work and Dr. H. Kokawa, Tohoku University (Tohoku, Japan), for performing the FESEM/XRD analyses of our welds.

REFERENCES

1. S.P. Murarka, R.J. Gutmann, A.E. Kaloyeros, and W.A. Landford: *Thin Solid Films*, 1993, vol. 236, pp. 257-66.
2. M.A. Wojcicki and R.J. Pryputniewicz: *ICALEO 1996 Laser Materials Processing*, Detroit, MI, Oct. 14–17, 1996, Laser Institute of America, Orlando, FL, pp. 84-92.
3. M.A. Wojcicki and R.J. Pryputniewicz: *1997 Proc. 47th Electronic Components & Technology Conf.*, San Jose, CA, May 18–21, 1997, IEEE, Piscataway, NJ, pp. 905-10.
4. J.H. Scheel: *Canadian Copper/Cuivre Canadien*, 1995, No. 134, pp. 4-5.
5. K. Shimizu and K. Hashimoto: *Fujitsu Sci. Technol.*, 1992, vol. 28 (3), pp. 310-15.
6. H. Lambilly and H. Keser: *IEEE Trans. Compon. Hybrids Manuf. Technol.*, 1993, vol. 16 (4) pp. 412-17.
7. F. Lechuga, E. Tyszka, J. Ramos, M. Bosman, and C. Timmermans: *ICALEO '99*, San Diego, CA, Nov. 15–18, 1999, Laser Institute of America, Orlando, FL, 1999, pp. D197-D205.
8. J.A. Ramos and F. Lechuga: *Proc. 19th ICALEO, Laser Materials Processing*, Dearborn, MI, Oct. 2–5, 2000, H. Hugel, A. Matsunawa, and J. Mazumder, eds., Laser Institute of America, Orlando, FL, 2000, vol. 89, pp. C62-C71.
9. W.W. Duley: *Laser Welding*, John Wiley & Sons, Inc., New York, NY, 1999.
10. H. Gouveia: *Proc. Latin American Regional Welding Congress*, Rio de Janiero, Apr. 4–10, 1992, Associacao Brasileira de Soldagem, Sao Paulo, Brazil, 1992, vol. 1, pp. 319-36.
11. H. Gouveia, J. Norrish, and L. Quintino: *Weld. Rev. Int.*, 1994, vol. 13 (2), pp. 266, 268-269, and 272-273.
12. H. Gouveia, I. Richardson, P. Kapadia, J. Dowden, and R. Ducharme: *ICALEO '94, Laser Materials Processing*, Orlando, FL., Oct. 17–20 2000, T.D. McCay, A. Matsunawa, and H. Hugel, eds., Laser Institute of America, Orlando, FL, 1994, vol. 79, pp. 480-89.
13. H.N. Gouveia: Ph.D. Thesis, Cranfield University, Bedfordshire, U.K., 1994.
14. M. Dell'erba: *Opt. Laser Technol.*, 1985, vol. 17 (5) pp. 261-62.
15. M. Dell'Erba, P. Sforza, G. Chita, and L. Cento: *Proc. 5th Int. Congress on Applications of Lasers and Electro-Optics, ICALEO '86*, Arlington, VA, Nov. 10–13, 1986, C.M. Banas, and G.L. Whitney, eds., Laser Institute of America, Orlando, FL, 1986, pp. 57-62.
16. G. Daurelio, and G. Giorleo: *Mater. Manuf. Processing*, 1991, vol. 6 (4) pp. 577-603.
17. H.N. Bransch, D.C. Weckman, and H.W. Kerr: *Weld. J.*, 1994, vol. 73 (6) pp. 141s-151s.
18. A. Matsunawa, S. Katayama, and K. Nishizawa: *Welding, Joining, Coating and Surface Modification of Advanced Materials*, Dalian, China, Sept. 1–2, 1994, Gansu University of Technology, Lanzou, Gansu, China, 1994, pp. 1-6.
19. E. Biro, Y. Zhou, D.C. Weckman, and K.J. Ely: *J. Laser Appl.*, 2001, vol. 13 (3) pp. 96-104.
20. *The Merck Index*, M. Windholz, ed., Merck & Co., Inc., Rahway, NJ, 1983.
21. G. Vander Voort: *Metallography, Principles and Practice*, McGraw-Hill, Inc., New York, NY, 1984.
22. H. Kokawa: Tohoku University, Tohoku, Japan, private communication, 2001.
23. W. Kurz and R. Trivedi: *Metall. Mater. Trans. A*, 1996, vol. 27A, pp. 625-34.
24. I. Ursu, L. Nanu, I.N. Mihăilescu, L.C. Nistor, V.S. Teodorescu, A.M. Prokhorov, V.I. Konov, and N.I. Chapliev: *J. Phys. Lett.*, 1984, vol 45 (14), pp. L-737-L-740.
25. I. Ursu, L.C. Nistor, V.S. Teodorescu, I.N. Mihăilescu, L. Nanu, A.M. Prokhorov, N.I. Chapliev, and V.I. Konov: *Appl. Phys. Lett.*, 1984, vol. 44 (2), pp. 188-89.
26. T. Tanaka: *Jpn. J. Appl. Phys.*, 1979, vol. 18 (6) pp. 1043-47.
27. J. Xie, A. Kar, J.A. Rothenflue, and W.P. Latham: *J. Laser Appl.*, 1997, vol. 9(2), pp. 77-85.
28. J.T. Liu, D.C. Weckman, and H.W. Kerr: *Metall. Trans. B*, 1993, vol. 24B (6), pp. 1065-76.
29. D.C. Weckman, H.W. Kerr, and J.T. Liu: *Metall. Mater. Trans. B*, 1997, vol. 28B, pp. 687-700.
30. C.J. Nonhof: *Material Processing with Nd-Lasers*, Electrochemical Publications Ltd. Ayr, Scotland, 1988.
31. *Oxide Handbook*, 2nd ed., G.V. Samsonov, ed., IFI/Plenum Data Company, New York, NY, 1982.
32. *Metals Handbook*, 10th ed. vol. 2, *Properties and Selection: Nonferrous Alloys and Special-Purpose Materials*, ASM INTERNATIONAL, Materials Park, OH, 1990.